Some TDMA and OFDM/CDMA receiver structures for communication over the return path of the CATV network

Mark Van Bladel, Heidi Steendam, Teresa Marongiu and Marc Moeneclaey
Communication Engineering Lab, University of Ghent, Belgium

Abstract

This paper deals with the derivation and comparison of some promising TDMA and OFDM/CDMA receiver structures for communication over the return path channel of the cable TV (CATV) network. Regarding TDMA, it is shown that the performance substantially improves by using equalization. Given the slowly varying, frequency selective nature of the ingress noise, OFDM seems an interesting possible access technique to employ. Here it is considered in combination with CDMA. With respect to the performance in terms of SNR at the input of the decision device, the TDMA structure gives better results than the OFDM/CDMA schemes. Also with respect to design complexity TDMA seems more interesting.

1. Introduction

Telecom operators experience more and more competition these days from cable TV operators when it comes to offering new telecommunication services. One can hereby think of fast internet, home shopping, banking, video on demand, telephony services etc... In order to allow for this type of applications the network configuration should evolve from a coaxial to a hybrid fiber coax (HFC) structure.
In the HFC architecture optical node units (ONU) are connected to the headend by means of single mode optical fiber, while the part between the ONU and a group of subscribers is over coaxial cable. This latter part of the structure is implemented as a tree and branch network. This network structure is now being modified to allow for bidirectional services. The return path must also be equipped with amplifiers. In general unity gain is desired from the first return amplifier as seen coming from the subscriber to the ONU. The scheme described here is shown in Figure 1.

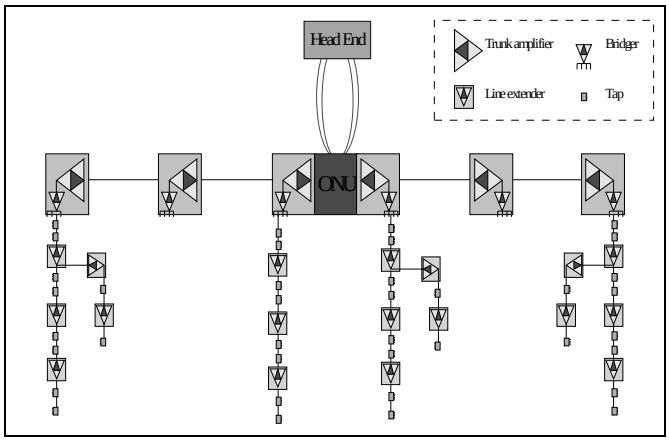

Figure 1 : typical HFC network structure

The CATV operator can choose which frequency band to use for the return path for the interactive services as well as the number of channels and the channel bandwidth. Some operators only want to use the spectrum between 5 and 35 MHz, whereas others go from 5 to 60 MHz. Anyway, in this paper results are presented for channels of 1 and 2 MHz bandwidth and with several values for the central frequency.
Apart from the non-ideal channel transfer function (which is also different for every user), two very important impairments are encountered in this type of networks, namely ingress noise and impulse noise. Ingress noise is slowly-varying noise, originating from nonlinearities in the CATV system, from interference generated by a device at the subscriber location or from signals radiatively coupled to the return path from outside the network. Impulse noise can be caused by a whole range of phenomena. It can be generated by naturally occurring sources (like lightning) and man-made sources (engine ignitions, power switching,...). It is assumed that most of the impulse noise can be counteracted by employing Forward Error Correction [1].
Various multiple access techniques can be considered to establish reliable communications over HFC networks. There has recently been an increasing interest in using multi-carrier spread-spectrum (MC-SS) techniques for high data rate applications [2-4]. An example of a MC-SS technique is the combination of orthogonal frequency division multiplexing (OFDM) and code division multiple access (CDMA). The combination of OFDM and CDMA can be expected to give good results because the peaks in the ingress noise spectra affect only a part of the carriers. As the CDMA part spreads the data symbols of the different users over the carriers, all users can transmit with comparable performances. The performance will also depend on the number of active users in the system. In this paper however, a fixed number of users is always considered.
Hereafter, the performance on the return path is compared with that of TDMA. In a TDMA system each channel is shared by many users, whom are assigned time slots to in order to send their information packets. As the signal-to-total noise ratio is determined by the total quantity of ingress noise within the channel bandwidth and by intersymbol interference, the performance of the TDMA system is user-independent.
The organization of the rest of the paper is as follows. Section 2 describes the derivation of a TDMA receiver structure and shows the benefit equalization can bring. In section 3 the basic OFDM/CDMA receiver scheme is presented. We also discuss the influence on the performance of adding certain filters to the scheme. Section 4 deals with the comparison between the TDMA and OFDM/CDMA receiver structures derived in previous sections in terms of performance and complexity. Finally, some conclusions are drawn in section 5.

2. Some TDMA receiver structures

In this section we shall discuss the benefits and drawbacks of some TDMA receiver schemes. The numerical results presented in this section are all obtained with the channel transfer function whose amplitude (deviation from the mean value) is given in Fig. 2. In the simulations this function is normalized, such that at the input of the receiver filter the signal has a power spectral density of -70 dBm/Hz. The ingress noise is modeled as coloured Gaussian noise with a power spectrum equal to the measured spectrum shown in Fig. 3. Note that this is a worst case noise spectrum : measurements were carried out during 24 hours and the values in the figure show the levels exceeded during only 0.1 % of the time.

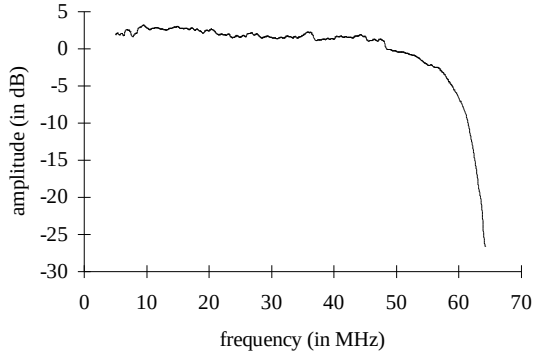

Figure 2 : amplitude transfer function

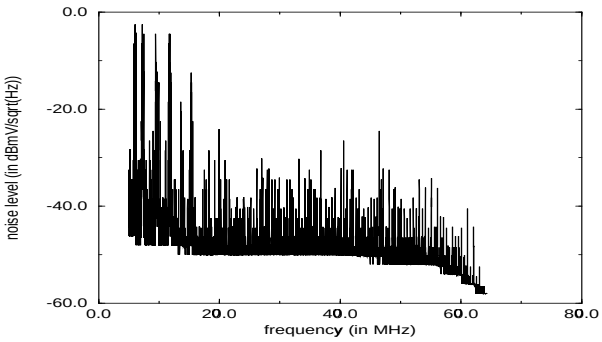

Figure 3 : ingress noise spectrum

Consider now the receiver structure depicted in Fig. 4a. The transmit filter is a square root raised cosine filter. The receiver filter is matched to both the channel, the ingress noise spectrum and the transmit pulse. This structure yields the theoretical optimal ratio of useful signal power P_s to noise power P_n at the input of the decision device (matched filter bound). Table 1 shows this optimal P_s/P_n for some channels, as well as the ratio of P_s to the intersymbol interference power P_{isi}. The calculations were done with a roll-off factor of 0.3. In the fourth column the total ratio $P_s/(P_{isi}+P_n)$ is given.

Note that the transmission of uncoded QPSK over an AWGN channel with a BER < 10^{-3} requires a E_s/N_o ratio of at least 9.8 dB. A bit error rate of 10^{-3} before channel coding corresponds to a BER of about 10^{-8} after coding.

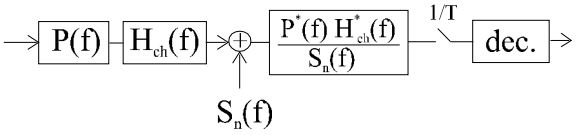

Figure 4a

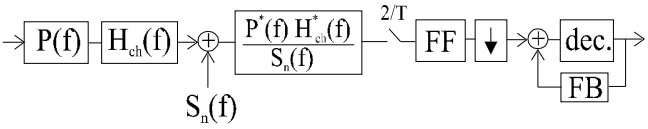

Figure 4b

channel (MHz)	P_s/P_n (dB)	P_s/P_{isi} (dB)	$P_s/(P_{isi}+P_n)$ (dB)
9 - 11	22.3	0.8	0.8
13 - 14	26.7	7.1	7.0
21 - 23	29.1	11.3	11.3
47 - 48	29.9	12.4	12.3
50 - 52	30.5	11.3	11.3

Table 1

Given the relatively flat shape of the transfer function, the ISI is mainly caused by the receiver filter. This high amount of ISI makes any communication virtually impossible. In order to increase the P_s/P_{isi} ratio we add decision feedback equalization to the scheme (Fig. 4b). Sampling is performed at twice the symbol rate. The forward filter is implemented as a fractionally spaced filter. At the output of the forward filter a decimation to the symbol rate takes place. The equalizer filters reduce the effect of the ISI, but at the same time the P_s/P_n ratio at the input of the decision device also decreases. Some numerical results for this case are summarized in Table 2.

channel (MHz)	Equalizer (FF/FB)	P_s/P_n (dB)	P_s/P_{isi} (dB)	$P_s/(P_{isi}+P_n)$ (dB)
9 - 11	50/25	17.3	6.2	5.9
	50/100	17.6	7.8	7.4
	∞ / ∞	16.9	∞	16.9
13 - 14	25/50	22.5	15.6	14.8
	50/100	22.1	19.6	17.7
	∞ / ∞	25.1	∞	25.1
21 - 23	50/25	24.8	18.3	17.5
	50/100	25.1	20.4	19.1
	∞ / ∞	28.8	∞	28.8
47 - 48	25/50	27.1	21.1	20.1
	50/100	25.8	25.6	22.7
	∞ / ∞	29.7	∞	29.7
50 - 52	25/50	28.4	16.5	16.2
	50/100	27.7	19.4	18.8
	∞ / ∞	30.3	∞	30.3

Table 2

For each channel the figures are given for a few lengths of feedforward and feedback filter. The DFE yields a gain of a few dB for the lower frequency channels, but even long equalizer filters cannot do much about the high ISI levels. The figures are still far from those we obtain with infinite length filters. In channels less affected by ingress the increase in $P_s/(P_{isi}+P_n)$ is larger. The results given for the channels between 9-11 and 21-23 MHz clearly demonstrate the importance of the feedback filter.

The receiver filter transfer function in Fig. 4 is quite complex and, as was discussed, a lot of ISI is introduced in this way. Therefore we now consider the receiver structure in Fig. 5. The receiver filter is a fixed filter matched to the transmitted pulse.

Results are given in Table 3. The relatively flat amplitude characteristic in Fig. 2 now gives rise to high P_s/P_{isi} ratios in all cases. In frequency bands not too heavily affected by ingress, good values for P_s/P_n are obtained as well. Communication over channels in the frequency band below 15 MHz still remains problematic in presence of a heavily peaked ingress spectrum like that of Fig. 3.

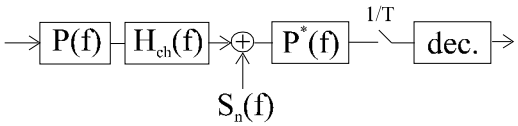

Figure 5

channel (MHz)	P_s/P_n (dB)	P_s/P_{isi} (dB)	$P_s/(P_{isi}+P_n)$ (dB)
9 - 11	2.5	32.8	2.5
13 - 14	14.9	40.3	14.8
21 - 23	27.6	47.9	27.6
47 - 48	27.5	39.8	27.2
50 - 52	29.7	42.8	29.5

Table 3

Attempting to obtain higher P_s/P_n ratios, we bring into the scheme of Figure 5 the decision feedback equalizer already shown in Fig. 4b. Sampling is again performed at 2/T. As can be read from Table 4, even with a feedforward and a feedback filter as short as 10 taps we obtain an increase of more than 10 dB. Comparing the figures for the channels 13-14 MHz and 9-11 MHz with those in Table 3, it is clear that the equalizer coefficients are adjusted such that in the first place they compensate for the noise; as a matter of fact, for the channel between 9 and 11 MHz the P_s/P_{isi} ratio has even decreased. The feedback filter proves to be very useful to compensate for the (postcursor) ISI introduced by the peaks in the ingress spectrum. For the channels that already had a good $P_s/(P_n+P_{isi})$, the improvement is relatively limited. The influence of the feedback filter has become less prominent in this case.

channel (MHz)	equalizer (FF/FB)	P_s/P_n (dB)	P_s/P_{isi} (dB)	$P_s/(P_{isi}+P_n)$ (dB)
9 - 11	10/10	14.2	21.7	13.5
	50/100	16.2	24.9	15.7
13 - 14	10/10	22.9	41.7	22.8
	50/100	24.4	49.7	24.4
21 - 23	10/10	28.0	53.1	28.0
	50/100	28.5	62.2	28.5
47 - 48	10/10	28.7	54.1	28.7
	50/100	29.0	61.1	29.0
50 - 52	10/10	29.8	59.2	29.8
	50/100	30.1	70.8	30.1

Table 4

3. Some OFDM/CDMA receiver structures

The basic transceiver structure of the OFDM/CDMA combination is shown in Figure 6. At the receiver side, the data symbols are first correlated with orthogonal CDMA sequences and then spread over the orthogonal OFDM carriers. The transmit filter P(f) is a square root raised cosine filter with respect to the interval T/N, N referring to the number of users and T the duration of the OFDM symbol. The receiver filter is matched to the transmit pulse. We assume a guard interval is inserted as a cyclic prefix, such that no inter-symbol interference occurs. With the channel transfer function of Figure 2, a guard interval of 8 samples is sufficient for all the channels we are considering. The main noise contributions are multi-user interference (MUI), due to the loss of orthogonality between the different users, and ingress noise. Simulations were done in the same circumstances as for the TDMA structures. The number of users N equals 256.

Table 5 shows the ratio of the useful signal power P_s to the MUI power P_{MUI} at the input of the decision device, as well as the ratio of P_s to the ingress noise power P_n and the total ratio $P_s/(P_{MUI}+P_n)$. The loss of orthogonality in this basic structure is caused only by the channel characteristics. As the channel transfer function is relatively flat, ingress noise is the dominant noise mechanism.

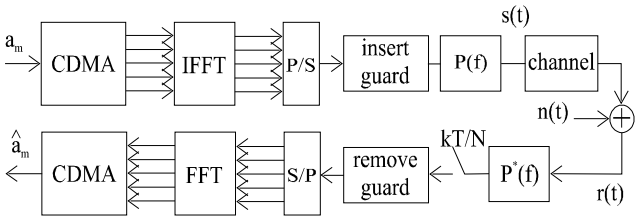

Figure 6

channel (MHz)	P_s/P_{MUI} (dB)	P_s/P_n (dB)	$P_s/(P_{MUI}+P_n)$ (dB)
9-11	26.8	1.4	1.3
13-14	31.6	13.8	13.7
21-23	42.0	26.5	26.4
47-48	31.6	27.1	25.8
50-52	36.9	28.5	27.9

Table 5

To improve the system performance, a filter is inserted as shown in Figure 7. It can be proven that the filter which optimizes the total ratio $P_s/(P_{MUI}+P_n)$, contains N^2 coefficients only depending on the channel characteristics and the ingress noise. To reduce the complexity of this filter, an alternative filter, containing only N coefficients, is proposed in Figure 8. This filter can be seen as a frequency domain equalizer,

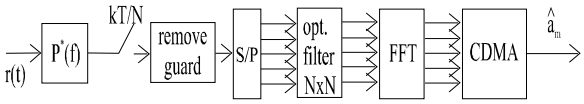

Figure 7

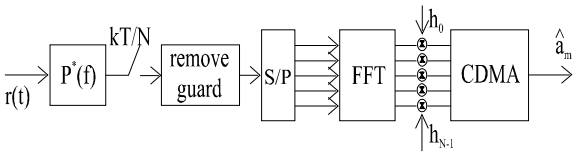

Figure 8

Tables 6 and 7 summarize the results for the filter of Figure 8 optimizing the P_s/P_{MUI} ratio and for the one that optimizes the P_s/P_n ratio, respectively. When maximizing the P_s/P_{MUI} ratio, a huge amount of ingress noise will obstruct reliable communication, and optimizing the P_s/P_n ratio will engender a high amount of MUI, as the used filter strongly affects the orthogonality between the users.

channel (MHz)	P_s/P_{MUI} (dB)	P_s/P_n (dB)	$P_s/(P_{MUI}+P_n)$ (dB)
9-11	50.5	0.9	0.9
13-14	34.3	13.7	13.7
21-23	63.2	26.5	26.5
47-48	34.2	27.1	26.3
50-52	60.1	28.5	28.5

Table 6

channel (MHz)	P_s/P_{MUI} (dB)	P_s/P_n (dB)	$P_s/(P_{MUI}+P_n)$ (dB)
9-11	0.5	18.5	0.5
13-14	6.8	25.4	6.7
21-23	10.6	27.7	10.5
47-48	11.4	28.7	11.3
50-52	11.2	29.2	11.2

Table 7

The performance of the filters shown in Figures 7 (a) and 8 (b), that maximize $P_s/(P_{MUI}+P_n)$, can be found in Table 8. As can be derived from the results in Table 8, we find that, although there is an enormous increase in complexity of the filter shown in Figure 7 compared to the alternative filter of Figure 8, the gain in the ratio $P_s/(P_{MUI}+P_n)$ is small.

channel (MHz)	filter	P_s/P_{MUI} (dB)	P_s/P_n (dB)	$P_s/(P_{MUI}+P_n)$ (dB)
9-11	a	10.0	10.1	7.0
	b	9.8	9.3	6.6
13-14	a	20.6	18.0	16.1
	b	20.4	17.9	16.0
21-23	a	51.3	26.5	26.5
	b	51.8	26.5	26.5
47-48	a	48.1	27.1	27.1
	b	34.0	27.1	26.3
50-52	a	59.9	28.5	28.5
	b	57.2	28.5	28.5

Table 8

A comparison of the figures in Tables 5 and 8 shows us that in regions highly affected by ingress noise the P_s/P_n ratio increases and at the same time, the P_s/P_{MUI} ratio decreases. For channels in the frequency band under 15 MHz reliable communication remains problematic, while for channels above 15 MHz, where the ingress spectrum is less peaked, a good signal to total noise ratio is obtained.

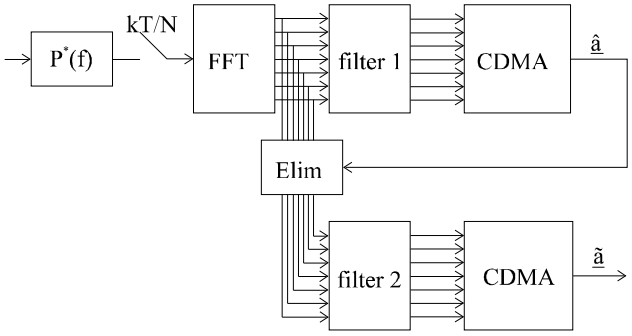

Figure 9

As the ingress noise can not be influenced by the system, an additional improvement of the performance can only be achieved by reducing the multi-user interference. In Figure 9, a feedback section was entered in the structure shown in Figure 8, eliminating the multi-user interference. Assuming perfect decisions, the signal after elimination is still disturbed by the ingress noise and needs an additional filter to diminish the effect of the ingress. Analog considerations as made for the filter of Figure 8 allow to implement this second filter as a filter with N coefficients, which need to be optimized to ingress only, as all multi-user interference is eliminated. Table 9 shows the results obtained with elimination of the multi-user interference.

channel (MHz)	P_s/P_{MUI} (dB)	P_s/P_n (dB)	$P_s/(P_{MUI}+P_n)$ (dB)
9-11	∞	18.5	18.5
13-14	∞	25.4	25.4
21-23	∞	27.7	27.7
47-48	∞	28.7	28.7
50-52	∞	29.2	29.2

Table 9

Comparing the results in Tables 8 and 9 we notice a major performance improvement for the channels severely affected by ingress noise. However, for channels disturbed by less peaked ingress, only a marginal gain in performance is obtained notwithstanding the increased complexity of the structure.
In practice, all filters are implemented as adaptive filters to meet the variation in time of the ingress noise. The dependency of the system performance on the number of carriers was not examined. However, it can be expected that increasing N, considering a fixed used bandwidth, will ameliorate the system performance of the structure shown in Figures 8 and 9. This can be explained by noticing that if N increases, the carrier spacing will decrease such that the noise experienced by a carrier behaves more white and makes the filter of Figure 8 converge to the complex filter of Figure 7. Nevertheless, it should be noted that increasing the number of carriers also leads to a rise in receiver complexity.

4. System comparison

Having another look at the figures in Tables 4 and 8, we immediately notice a difference in performance. Even for a TDMA structure with short equalizer filters, we find for the channels below 15 MHz a signal-to-noise ratio more than 6 dB higher than in Table 8. In other words, it is mandatory to take measures to eliminate the multi-user interference in the OFDM/CDMA scheme in order to obtain signal-to-overall interference ratios more or less similar to that for TDMA (see Figure 9 and Table 9). In that case the OFDM/CDMA scheme gives even better results than the TDMA structure for channels impaired by strong ingress noise peaks.
Let us compare now the system complexity. In the TDMA scheme with equalization one obtains good results with relatively short filters. The basic structure of the OFDM/CDMA scheme is clearly more complex (multiplication with PN sequence, (I)FFT, …). Concerning the adaptive filtering/equalization, we have already indicated that the much simpler structure of Fig. 8 gives almost as good results as the filter with N^2 coefficients in Fig. 7. With the filter of Fig. 8 there are N multiplications per OFDM symbol, where N is the number of users. The structure depicted in Figure 9 is definitely the most complex one. Filters 1 and 2 in the figure can be N-tap filters, whereas the filter to eliminate the MUI must be a NxN filter. Typical values for N range from 64 to 512. For TDMA good results were obtained with equalizer filters with 50 taps.

5. Conclusions

In this paper some receiver schemes for communication over the return path of the CATV network were discussed. A TDMA structure suitable for this type of communication was derived. We indicated the profit decision feedback equalization could bring in combating the effect of the peaks in the ingress noise spectrum. Next some structures were considered where the chips of a PN sequence are put on the carriers of an OFDM structure. Filters to compensate for the ingress noise and multi-user interference can improve the performance. However, it was shown that several adaptive filters are required to obtain a performance comparable to that of the TDMA solution. The main advantage of the TDMA scheme is its much higher simplicity from an implementation point of view.

Acknowledgment

The authors would like to express their gratitude to the Flemish government by means of the IWT and the other partners in the Hybrid Fiber Coax Systems project, i.e. the research department of Alcatel Alsthom in Belgium, Barco, Integan and the Intec department of the University of Ghent. Part of this work has been carried out within the framework of the European ACTS Interact project. The first author therefore would also like to thank the partners in this project, namely Alcatel SESA (E), Barco (B), Bosch (D), CCETT (F), EBU (B), Integan (B), ITC (GB), Nozema (NL), Retevision (E), SAT (F), TBS (F), TDF (F) and UPM (E). The last author gratefully acknowledges the financial support from the Flemish Fund for Scientific Research (FWO-Vlaanderen).

References

[1] “CATV Return Path Characterization for Reliable Communications”, C. Eldering, N. Himayet and F. Gardner, IEEE Communications Magazine, August 1995, pp.62-69
[2] “Wideband CDMA System for Personal Radio Communication”, Fukusawa , A., Sato , T., Takizawa, Y. et al., IEEE Comm. Mag., vol. 34, no. 10, Oct 96, pp. 116-123
[3] “New Concepts and Technologies for Achieving Highly Reliable and High-Capacity Multimedia Wireless Communications Systems”, Morinaga, N., Nakagawa , M., Kohno, R., IEEE Comm. Mag., vol. 35, no. 1, Jan 97, pp. 34-40
[4] “Performance of Orthogonal Multicarrier CDMA in a Multipath Fading Channel”, Sourour , E.A., Nakagawa , M., IEEE Trans. on Comm., vol. 44, no. 3, Mar 96, pp. 356-367